Biochemical and Biophysical Research Communications 452 (2014) 328–333

Contents lists available at ScienceDirect

Biochemical and Biophysical Research Communications

journal homepage: www.elsevier.com/locate/ybbrc

MIG-10 (Lamellipodin) stabilizes invading cell adhesion to basement membrane and is a negative transcriptional target of EGL-43 in *C. elegans*

Lin Wang [a], Wanqing Shen [a], Shijun Lei [a], David Matus [c], David Sherwood [d], Zheng Wang [a,b,*]

[a] Center for Tissue Engineering and Regenerative Medicine, Union Hospital, Tongji Medical College, Huazhong University of Science and Technology, Wuhan, Hubei 430022, China
[b] Department of Surgery, Union Hospital, Tongji Medical College, Huazhong University of Science and Technology, Wuhan, Hubei 430022, China
[c] Department of Biochemistry and Cell Biology, Stony Brook University, Stony Brook, NY 11794, USA
[d] Department of Biology, Duke University, 124 Science Drive, Box 90388, Durham, NC 27708, USA

ARTICLE INFO

Article history:
Received 4 August 2014
Available online 19 August 2014

Keywords:
MIG-10
Lamellipodin
EGL-43
Anchor cell
Cell invasion

ABSTRACT

Cell invasion through basement membrane (BM) occurs in many physiological and pathological contexts. MIG-10, the *Caenorhabditis elegans* Lamellipodin (Lpd), regulates diverse biological processes. Its function and regulation in cell invasive behavior remain unclear. Using anchor cell (AC) invasion in *C. elegans* as an *in vivo* invasion model, we have previously found that *mig-10*'s activity is largely outside of UNC-6 (netrin) signaling, a chemical cue directing AC invasion. We have shown that MIG-10 is a target of the transcription factor FOS-1A and facilitates BM breaching. Combining genetics and imaging analyses, we report that MIG-10 synergizes with UNC-6 to promote AC attachment to the BM, revealing a functional role for MIG-10 in stabilizing AC-BM adhesion. MIG-10 is also required for F-actin accumulation in the absence of UNC-6. Further, we identify *mig-10* as a transcriptional target negatively regulated by EGL-43A (*C. elegans* Evi-1 proto-oncogene), a transcription factor positively controlled by FOS-1A. The revelation of this negative regulation unmasks an incoherent feedforward circuit existing among *fos-1, egl-43* and *mig-10*. Moreover, our study suggests the functional importance of the negative regulation on *mig-10* expression by showing that excessive MIG-10 impairs AC invasion. Thus, we provide new insight into MIG-10's function and its complex transcriptional regulation during cell invasive behavior.

1. Introduction

Cell invasion takes place in diverse contexts, including organogenesis, morphogenesis, immune surveillance, wound healing, and regeneration [1]. A common barrier the invading cells have to navigate through is basement membrane (BM), a dense, 50–100 nm thick, sheet-like structure consisting of highly-crosslinked and self-assembled glycoproteins and proteoglycans [2]. Defects in the cell invasive machinery contribute to various human diseases, including asthma, pre-eclampsia [3,4], and importantly, cancer metastasis, which accounts for 90% mortality in solid cancers [5]. Thus, understanding how cells invade through BM in physiological contexts could help identify novel targets for treating these diseases.

Cell invasion through BM requires the coordination of multiple interlinked steps beginning with establishing direct contact between cells and their invading target, BM. During this establishment, diverse cellular processes, such as cytoskeleton reorganization [6] and gene transcription [7,8], are precisely regulated towards successful BM breaching.

Anchor cell (AC) invasion in *Caenorhabditis elegans* has been developed to be an *in vivo* invasion model (Fig. 1A) [7,9,10]. During the L2/L3 larval stage of *C. elegans* hermaphrodite development, the AC, a highly specialized gonadal cell, invades through the gonadal and vulval BMs and contacts the central primary vulval precursor cells (1° VPC). This invasion initiates the connection between the uterine and vulval cells [10]. Prior to invasion (1° VPC P6.p 1-cell stage), UNC-6 (netrin) secreted from the ventral nerve cord (VNC) and integrin signaling from within the AC synergistically promote the formation of a specialized F-actin-rich invasive membrane domain with polarized actin regulators at the basal membrane of the AC in contact with the BM [9]. Approximately five hours later, when the P6.p cell gives rise to two daughter cells (2-cell stage), the AC initiates invasion by generating invasion protrusions. The transcription factor FOS-1A is required for breaching and further removing BM [7]. AC invasion is completed by the time the P6.p descendants divide again, generating four granddaughter

* Corresponding author at: Department of Surgery, Union Hospital, Tongji Medical College, Huazhong University of Science and Technology, Wuhan, Hubei 430022, China.
E-mail address: wzwangzheng@gmail.com (Z. Wang).

http://dx.doi.org/10.1016/j.bbrc.2014.08.049
0006-291X/

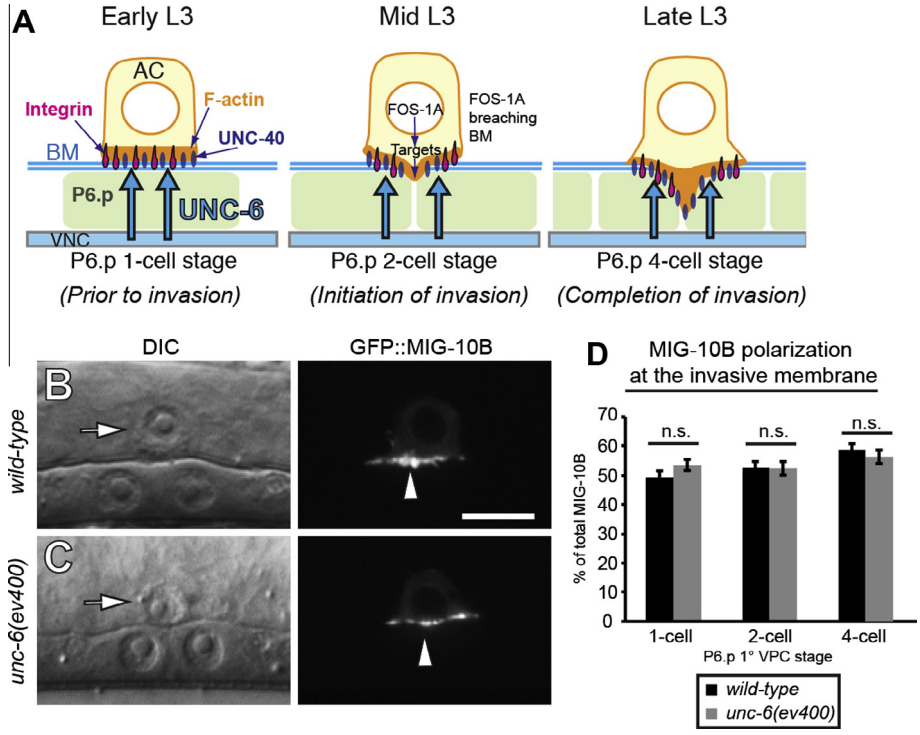

Fig. 1. Schematics of AC invasion and localization of MIG-10B in *unc-6* mutants. Anterior is left; ventral is down; and arrows point to the AC in this and all other figures. (A) A schematic diagram illustrates AC invasion in *C. elegans*. In the early L3 larva the AC is attached to the basement membrane (BM, light blue) over the primary vulval precursor cell (1° VPC) (light green, P6.p 1-cell stage, left). At this time UNC-6 (netrin) (blue arrows) secreted from the ventral nerve cord (VNC) polarizes its receptor UNC-40 (blue ovals) and F-actin (orange) to the invasive cell membrane in contact with BM in the presence of integrin (magenta). During the mid-L3 stage, after the P6.p cell divides (P6.p 2-cell stage, middle), the AC breaches the BM and generates an invasive protrusion that invades between the two central 1° VPC granddaughter cells by the late L3 (P6.p 4-cell stage, right). The transcription factor FOS-1A promotes BM breaching. UNC-40 (DCC) mediates protrusion formation. (B and C) DIC images (left) and corresponding fluorescence (right). MIG-10B was similarly polarized at the AC's basal membrane (arrowheads) in the wild-type and *unc-6* mutants at the P6.p 2-cell stage. (D) Quantification of MIG-10B polarization at the P6.p 1-, 2- and 4-cell stages in wild-type animals and *unc-6* mutants ($n \geqslant 10$ per stage per genotype, Student's *t*-test). In this and all other figures, *, $p < 0.05$; **, $p < 0.01$; ***, $p < 0.001$; n.s., not significant. Error bars, standard error of mean. Scale, 5 μm. (For interpretation of the references to color in this figure legend, the reader is referred to the web version of this article.)

cells (4-cell stage). At this time, the AC creates a gap in the BM the size of the AC.

C. elegans MIG-10 is a member of the MIG-10/RIAM/Lamellipodin (MRL) adaptor protein family that plays an important role in cell migration [11]. MIG-10 regulates axon guidance, neuronal migration [12], the clustering of vesicles at the synapse [13], and the outgrowth of the processes of the excretory cell [14]. In AC invasion, we have previously found that *mig-10* functions largely outside of *unc-6 (netrin)* signaling [15] in contrast to *mig-10* acting downstream of *unc-6* in axon guidance [12]. While MIG-10 polarization to the invasive membrane is dependent on the extracellular matrix receptor integrin heterodimers (INA-1/PAT-3), *mig-10* expression is positively controlled by FOS-1A, which regulates the expression of genes that promote BM breaching [15]. Given that *mig-10* acts redundantly with other FOS-1A target genes, *mig-10* was thought to help breach BM [15].

Here we report that MIG-10 synergizes with UNC-6 to promote AC attachment to the BM in a cell-autonomous manner prior to and throughout invasion. MIG-10 regulates F-actin accumulation in the absence of UNC-6. Moreover, EGL-43, a transcription factor downstream of FOS-1A, negatively regulates *mig-10* expression, which together with the known regulatory relationships between *fos-1* and *egl-43*/*mig-10* forms an incoherent (type I) feedforward transcriptional loop. Further, we suggest that the negative regulation on *mig-10* expression is functionally important as overexpressed MIG-10 disrupts AC invasion. Thus, we identify a functional role for MIG-10 in promoting cell-matrix adhesion in AC invasion and unveil a new layer of the complicated transcriptional regulation on *mig-10*.

2. Materials and methods

2.1. Worm handling and strains

Worms were reared under standard conditions at 15 °C, 20 °C, or 25 °C [16]. N2 Bristol strain was used as wild-type. We use a ">" symbol for linkages to a promoter and a "::" symbol for linkages that fuse open reading frames. The following alleles and transgenes were used: *qyIs57[cdh-3>mCherry::moeABD], qyIs183 [cdh-3>GFP::mig-10b;cdh-3>mCherry], sIs14214[mig-10b>GFP], cuwEx1[cdh-3>GFP::mig-10b(overexpressed; higher level); cdh-3> mCherry::moeABD]; cuwEx2[cdh-3>GFP::mig-10b(overexpressed; lower level); cdh-3>mCherry::moeABD].* Linkage Group: **LGII,** *rrf-3(pk1426)*; **LGIII**, *mig-10(ct41);* **LGX**, *unc-6(ev400).*

2.2. Microscopy, image acquisition, and image processing

Images were acquired using an Olympus BX53 microscope with a 100× UPlanSApo objective (NA 1.4) and a XM10 CCD camera controlled by cellSens Entry software (Olympus, Japan), or a Zeiss AxioImager microscope with a 100× Plan-APOCHROMAT objective (NA 1.4) and a Zeiss AxioCam MRm CCD camera controlled by Axiovision software (Zeiss Microimaging), or Zeiss AxioImager microscope with a 100× Plan-APOCHROMAT objective (NA 1.4) and a Yokogawa CSU-10 spinning disc confocal controlled by iVision software (Biovision Technologies). Acquired images were processed using ImageJ 1.40 and Photoshop CS5 (Adobe Systems). 3D reconstructions were generated from confocal z-stacks,

analyzed and exported using Imaris 7.4 (Bitplane). Graphs and figures were made using Adobe Illustrator CS5 (Adobe Systems).

2.3. Quantitative measurements of MIG-10B and F-actin polarization and the expression level of mig-10b transcriptional reporter

MIG-10B and F-actin polarization was determined as the percentage of the fluorescence intensity at the invasive membrane region over the total fluorescence intensity within the entire cell (nucleus excluded) using ImageJ 1.40. EGL-43 positively controls *cdh-3* promoter [17]. For quantifying F-actin polarity after *egl-43a* RNAi, the ACs that failed to invade and had mCherry::moeABD expression at the reasonable level for imaging were used for analysis. For quantifying *mig-10b>GFP* expression, the total fluorescence intensity within the ACs in *sIs14214[mig-10b>GFP]* animals that were treated with either L4440 control RNAi or *egl-43a* RNAi, was measured using ImageJ 1.40.

2.4. RNA interference

Double-stranded-RNA(dsRNA)-mediated gene interference was conducted by feeding larvae with bacteria expressing dsRNA using standard techniques [18]. To bypass *egl-43a* RNAi's early effect on AC/VU (anchor cell/ventral uterine) fate specification, synchronized L1-arrested larvae of *qyIs57*, *sIs14214[mig-10b>GFP]*, *rrf-3(pk1426),* and *rrf-3(pk1426);mig-10(ct41)* were grown for 2 h on regular OP50 bacteria at 20 °C before transferred to *egl-43a* RNAi plates.

2.5. Quantitative analysis of F-actin volume

F-actin volume was measured as previously described [19]. Briefly, confocal z-stacks of F-actin networks in the AC expressing the F-actin binding probe (mCherry::moeABD) were collected. 3D reconstructions of F-actin were built using these z-stacks in Imaris 7.4 (Bitplane). Isosurface renderings of mCherry::moeABD were created using Imaris "isosurface rendering" function by setting a threshold that outlined the dense F-actin network. Quantitative measurements were made for the volume of fluorescent intensity within these isosurface renderings [19].

2.6. Molecular biology and transgenic strains

The RNAi clone specifically targeting *egl-43a* was generated by PCR amplifying the unique coding region (1st bp–636th bp) of *egl-43a* cDNA. This fragment was inserted into the L4440 plasmid at *Xba*I and *Hind*III. Standard techniques were used to generate transgenic animals [20]. The constructs *cdh-3>GFP::mig-10b* [15] and *cdh-3>mCherry::moeABD* [9] were used to generate *cuwEx1* and *cuwEx2* transgenic animals (Table S1). Transgenic worms were created by co-injecting expression constructs with the transformation marker pPD#MM016B (*unc-119+*) and the co-injection marker (*myo-2>GFP*) into the germline of *unc-119(ed4)* mutants. These markers were injected with *Eco*RI-digested salmon sperm DNA and pBluescript II at 50 ng/μl as carrier DNA along with the expression constructs.

2.7. Statistics

Statistical analyses were performed using Student's *t*-test or Fisher's exact test as indicated in the text.

3. Results and discussion

3.1. MIG-10B remains polarized at the invasive membrane of the AC in unc-6 mutants

Among *mig-10*'s three different isoforms, *mig-10b* is the only isoform specifically expressed in the AC [15]. To further study MIG-10B's function in AC invasion, we first examined MIG-10B's localization in *unc-6* mutant ACs. *Mig-10b* expression was driven by the AC-specific promoter *cdh-3* (*qyIs183[cdh-3>GFP::mig-10b]*). At this expression level, AC invasion was not disturbed ($n = 20/20$ invaded at the P6.p 4-cell stage). In wild-type animals, approximately 50–55% of the total amount of MIG-10B was polarized at the AC's basal plasma membrane prior to and during AC invasion (Fig. 1B and D). MIG-10B was similarly polarized in *unc-6* mutants (Fig. 1C and D), indicating that MIG-10B polarization is independent of UNC-6, consistent with the majority of MIG-10B's activity outside of netrin signaling [15].

3.2. MIG-10B synergizes with UNC-6 to promote AC adhesion to the BM

Loss of *mig-10* alone causes mild invasion defects [15], suggesting that *mig-10* acts with other genes during invasion. We next examined AC invasion in the double null mutants *unc-6(ev400);mig-10(ct41)*. In *unc-6(ev400)* single mutants, all ACs attached to the BM at the P6.p 1-cell stage prior to the invasion (Fig. 2A and C). The ACs later started to detach from the BM staying afloat in the gonad. The percentage of detached ACs increased to 10% and 15% at the P6.p 2- and 4-cell stages, respectively (Fig. 2C), suggesting that UNC-6 promotes AC-BM adhesion during AC invasion. In contrast, *mig-10(ct41)* mutants had no phenotypic defects in AC-BM attachment. However, when *mig-10* was removed in *unc-6* mutants, AC detachment was observed at the P6.p 1-cell stage, revealing an early requirement for MIG-10B in stabilizing AC-BM attachment (Fig. 2B and C). AC detachment was later drastically increased by approximately 4–6 folds at the P6.p 2- and 4-cell stages (Fig. 2C), indicating a synergistic effect between MIG-10B and UNC-6 on mediating AC-BM adhesion during AC invasion. To determine MIG-10B's site of action in adhesion regulation, we expressed *mig-10b* under the AC-specific promoter *cdh-3* in *unc-6;mig-10* doubles. AC-specific expression of *mig-10b* rescued detachment and restored AC-BM association to the level similar to *unc-6* single mutants (Fig. 2C), suggesting a cell-autonomous role for MIG-10B in regulating adhesion. Together, these results reveal a progressively increased requirement for MIG-10B within the AC for AC-BM association in the absence of UNC-6.

Given that MIG-10B's polarized localization at the invasive membrane depends on integrin [15], MIG-10B may function within integrin signaling to regulate cell-matrix association. Interestingly, RIAM and Lamellipodin (Lpd), another two members of the MRL protein family, are able to activate integrin [21–23], but elicit opposing effects on adhesion [21]. Under simplified *in vitro* cell culture conditions, RIAM promotes cell adhesion, whereas Lpd reduces adhesion. Although it remains to be determined whether RIAM and Lpd also exert differential regulatory effects on adhesion *in vivo*, our results provide evidence supporting MIG-10B's *in vivo* role in promoting cell-matrix adhesion.

3.3. MIG-10B promotes F-actin accumulation in unc-6 mutants

Cell-matrix adhesion is tightly coupled with actin dynamics regulation [24]. To determine how loss of *mig-10* enhanced AC detachment from the BM, we examined MIG-10B's effect on F-actin in *unc-6* mutants. Consistent with the previous report [19], loss of

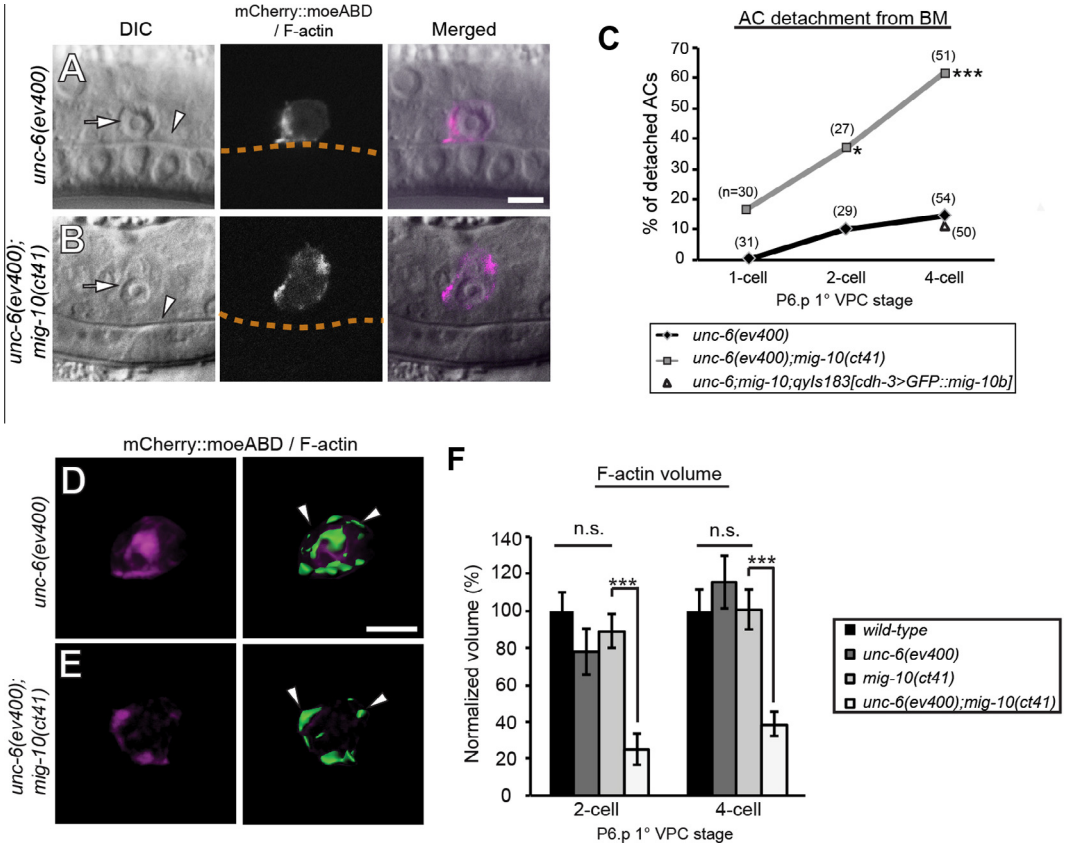

Fig. 2. Loss of *mig-10* enhances AC detachment from the BM and reduces F-actin accumulation in the absence of UNC-6. (A and B) DIC images (left), corresponding fluorescence (middle), and overlay (right). (A) In *unc-6* mutants the AC (visualized by F-actin binding probe *cdh-3>mCherry::moeABD*) failed to invade and attached to the intact BM (arrowheads; orange dotted line). (B) In *unc-6;mig-10* double mutants, the AC failed to invade and detached from the BM. (C) Quantification of AC detachment percentage in *unc-6* and *unc-6;mig-10* mutants at the P6.p 1-, 2- and 4-cell stages, and in *unc-6;mig-10;qyIs183* at the P6.p 4-cell stage. The total numbers of animals scored and significant differences are indicated (Fisher's exact test). (D and E) 3D reconstructions of confocal z-stacks from the ACs at the P6.p 4-cell stage. Fluorescence (left), overlay of fluorescence and corresponding F-actin networks rendered with isosurfaces (right). (D) In *unc-6* mutants F-actin (visualized by F-actin probe *cdh-3>mCherry::moeABD*) was mislocalized to the AC's apical-lateral membranes (arrowheads). (E) In *unc-6;mig-10* doubles F-actin remained mispolarized. The volume of F-actin was significantly reduced. (F) Quantification of the normalized total volume of F-actin in the wild-type (normalization control), *unc-6, mig-10, unc-6;mig-10* mutants at the P6.p 2- and 4-cell stages ($n \geqslant 15$ per stage per genotype). Significant differences are indicated (Student's *t*-test). (For interpretation of the references to color in this figure legend, the reader is referred to the web version of this article.)

unc-6 alone disrupted only F-actin polarity without affecting F-actin total amount in comparison to the wild-type (Fig. 2D and F; Fig. S1). While loss of *mig-10* in *unc-6* mutants did not further disrupt F-actin polarity (Fig. S1), it did reduce F-actin amount by 68% and 67% at the P6.p 2- and 4-cell stages, respectively (Fig. 2D–F), suggesting that MIG-10B promotes F-actin accumulation in *unc-6* mutant ACs, consistent with the MRL family proteins' role in regulating actin cytoskeleton [15]. Given this synergistic effect between MIG-10B and UNC-6, it is possible that MIG-10B is involved in regulating actin regulators downstream of UNC-6, such as *unc-34(Ena/VASP), mig-2/Rac, ced-10/Rac* [15], or other unidentified players. More importantly, this marked reduction in F-actin amount occurred concurrently with a significant enhancement in AC detachment, raising a possibility that MIG-10B mediates AC-BM adhesion through maintaining F-actin accumulation in the absence of UNC-6.

3.4. EGL-43A suppresses mig-10b expression and forms an incoherent (type I) feedforward loop (IFFL) with FOS-1A and MIG-10B

Although the synergistic effects between MIG-10B and UNC-6 suggest the downstream convergence that warrants future investigation, these effects also indicate that MIG-10B has the activity controlled by netrin-independent pathways. FOS-1A, a key transcription factor during AC invasion, controls a complicated gene regulatory network involving *mig-10* [15] and *egl-43* (a transcription factor [25]). To further investigate the interactions between *mig-10b* and the *fos-1* network components, we examined *egl-43's* effect on *mig-10b* expression using a reporter containing 5′ *cis*-regulatory elements (2.9 kb sequence immediately upstream of *mig-10b* start codon) to drive GFP [15]. *Egl-43*, the *C. elegans* Evi-1 proto-oncogene, encodes two different transcripts. The longer isoform *egl-43a* is transcriptionally controlled by FOS-1A and required for AC invasion, whereas the shorter isoform *egl-43b* is not regulated by FOS-1A [17]. The role of *egl-43b* in AC invasion is unclear because *egl-43b*'s open reading frame with 3′ UTR is contained in *egl-43a* (Fig. S2), making it difficult to down-regulate *egl-43b* without affecting *egl-43a* [17]. We thus specifically targeted *egl-43a* with an RNAi clone containing the sequence against the unique coding region of *egl-43a* (Fig. S2). The reduction in EGL-43A blocked AC invasion (Fig. 3A and B), consistent with the previous report [17]. Intriguingly, this reduction increased *mig-10b* expression prior to (approximately 2.5 folds for the p6.p 1-cell stage) and throughout AC invasion (2 folds for the p6.p 2- and 4-cell stages) (Fig. 3C). Moreover, while wild-type animals had *mig-10b* expression peaked at the P6.p 2-cell stage, *egl-43a* RNAi resulted in the early appearance of this peak at the P6.p 1-cell stage (Fig. 3C). Together, these results indicate that EGL-43A suppresses *mig-10b* expression and delays peaking of *mig-10b* expression.

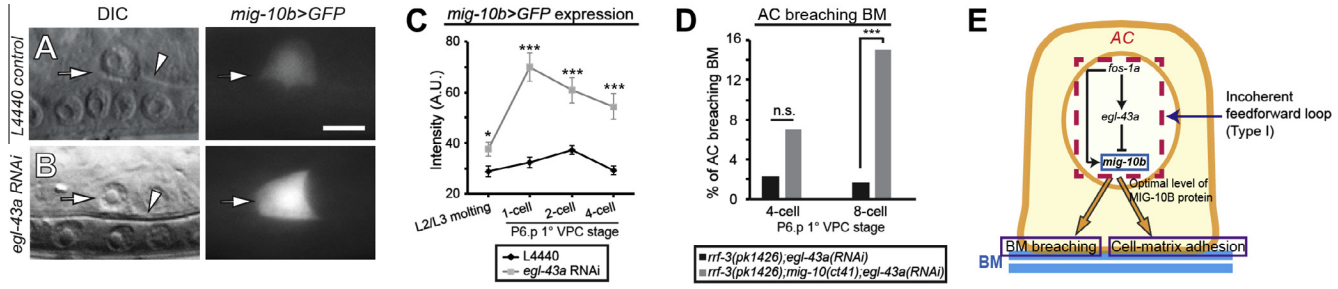

Fig. 3. EGL-43A negatively regulates *mig-10b* expression and forms an incoherent (type I) feedforward loop with FOS-1A and MIG-10B. (A and B) DIC images (left), corresponding fluorescence (right). (A) In the animal treated with L4440 control RNAi, the AC invaded normally at the P6.p 4-cell stage (arrowhead) and *mig-10b (mig-10b>GFP)* expression was detected in the AC. (B) RNAi targeting *egl-43a* resulted in AC invasion failure (arrowhead) and an increase in *mig-10b* expression in the AC. (C) Quantification of *mig-10b* expression at the L2/L3 transition, the P6.p 1-, 2-, and 4-cell stages in the animals treated with L4440 control RNAi and *egl-43a* RNAi ($n \geqslant 20$ per stage per treatment). (D) The percentage of the ACs that breached the BM at the P6.p 4- ($n = 85$ per genotype) and 8-cell ($n = 60$ per genotype) stages in *rrf-3* mutants and *rrf-3;mig-10* mutants treated with *egl-43a* RNAi. Significant differences are indicated (Fisher's exact test). (E) Within the AC, FOS-1A's positive transcriptional regulation on *egl-43a* (arrow), EGL-43A's negative transcriptional regulation on *mig-10b* (blunt arrow), and FOS-1A's positive transcriptional regulation on *mig-10b* (arrow), form an incoherent (type I) feedforward loop (boxed by red dashed lines). This loop may help maintain a stable, optimal level of *mig-10* expression required for effective AC-BM adhesion and AC breaching through BM (blue lines). (For interpretation of the references to color in this figure legend, the reader is referred to the web version of this article.)

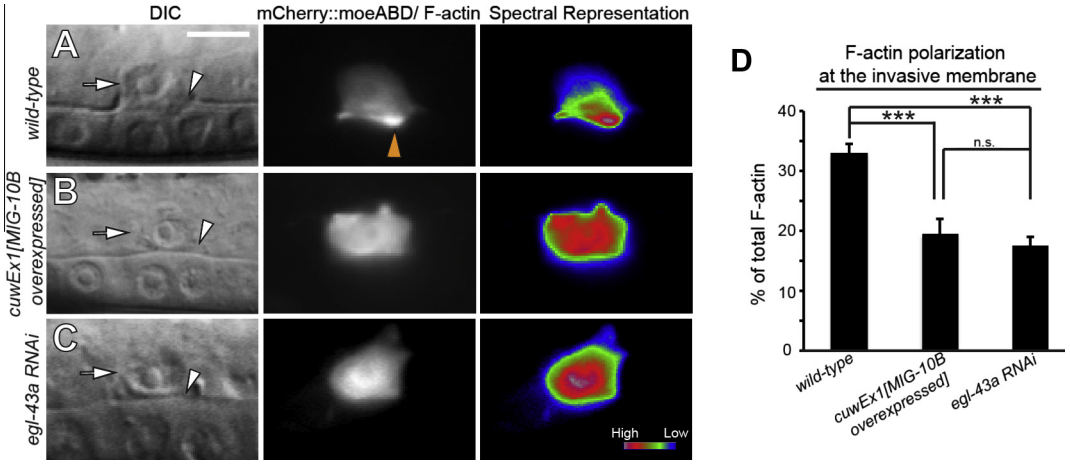

Fig. 4. Overexpression of *mig-10b* disrupts AC invasion and F-actin polarity. (A–C) DIC image (left), corresponding fluorescence (middle), and spectral representation of fluorescence images (right) at the P6.p 4-cell stage. (A) In wild-type animals the AC (arrow, expressing F-actin probe) invaded through BM (arrowhead) and polarized F-actin at the invasive membrane (yellow arrowhead). (B) In the AC overexpressing MIG-10B, the polarized localization of F-actin was loss. (C) In the animals treated with *egl-43a* RNAi, the AC failed to invade and lost F-actin polarized localization. (D) Quantification of F-actin polarization in the wild-type ACs, the ACs overexpressing *mig-10b* and the ACs in the animals treated with *egl-43a* RNAi at the P6.p 4-cell stage ($n \geqslant 10$ per genotype). Significant differences are indicated (Student's *t*-test). (For interpretation of the references to color in this figure legend, the reader is referred to the web version of this article.)

To test whether the enhanced *mig-10b* expression contributes to AC invasion failure caused by loss of *egl-43a*, we removed *mig-10* in *egl-43a* RNAi-treated *rrf-3* mutants that were used as an RNAi sensitive genetic background. Loss of *mig-10* suppressed invasion defects in *egl-43a* RNAi-treated animals (Fig. 3D), indicating that the aberrantly excessive MIG-10B contributes to AC invasion defects resulted from *egl-43a* RNAi. This incomplete rescue also suggests that the mechanisms independent of enhanced *mig-10b* expression exist accounting for *egl-43a* RNAi-mediated invasion failure.

Given that *fos-1a* positively regulates the expression of both *egl-43a* and *mig-10b* during AC invasion [15,17], the revelation of *egl-43a*'s negative regulation on *mig-10b* expression unmasks an incoherent (type I) feedforward loop (IFFL) (Fig. 3E), a common motif of gene regulatory networks [26], among *fos-1a*, *egl-43a* and *mig-10b* within the FOS-1A network. As the IFFL is thought to prevent the propagation of potentially harmful fluctuations in gene expression [27], this *fos-1a-egl-43a-mig-10b* loop may act to ensure *mig-10b* expression at a stable, optimal level for AC invasion.

3.5. Overexpression of mig-10b disrupts AC invasion and F-actin polarity

To determine whether the expression level of *mig-10b* is functionally critical to AC invasion, we overexpressed full-length *mig-10b* cDNA using AC-specific promoter *cdh-3* whose activity remains relatively constant throughout AC invasion [19]. Two transgenic lines expressing *mig-10b* at the low and high levels (2.6-fold difference in fluorescence intensity) were generated. 39% of the ACs ($n = 14/36$) with low *mig-10b* expression and 63% of the ACs ($n = 33/52$) with high expression failed to invade at the P6.p 4-cell stage, suggesting a potential correlation between the severity of invasion defects and *mig-10b* expression levels. These two MIG-10B overexpressed lines had a loss in F-actin polarity (Fig. 4B and D), indicating that *mig-10b* overexpression disrupts F-actin polarity. Supporting this, the *egl-43a* RNAi-treated animals where *mig-10b* expression was elevated exhibited a similar polarity loss (Fig. 4C and D). Although it was unclear how overexpressed MIG-10B led to F-actin polarity loss, these results indicate that excessive MIG-10B is detrimental to AC invasion, suggesting the

importance of a negative control on *mig-10b* expression. Such negative regulation may be realized partly through EGL-43A. Further, the negative regulation on *mig-10b* expression seems to be also required for other biological processes. In the monopolar neurons, such as AVM, *mig-10b* overexpression causes a multi-protrusive phenotype [12], impairing the unidirectional axon extension. It would be of interest to test whether *mig-10b* is also transcriptionally regulated in other biological processes in a manner similar to AC invasion.

4. Conclusion

Although MIG-10 (Lamellipodin) regulates diverse biological processes [12–14], *mig-10*'s function and regulation in cell invasive behavior are not fully understood. Using AC invasion in *C. elegans* as an *in vivo* model, we have found MIG-10B's synergistic role with UNC-6 in regulating AC-BM adhesion. MIG-10B's function in cell-matrix attachment is likely associated with MIG-10B promoting F-actin accumulation in the absence of UNC-6. The involvement of MIG-10B in AC-BM attachment extends the function of the FOS-1A transcription regulatory network beyond BM breaching. Further, we unveil *egl-43a*'s negative regulation on *mig-10b* expression and suggest the functional importance of the negative expression control on *mig-10b* during AC invasion. The identification of this negative regulatory link between *egl-43a* and *mig-10b* reveals the existence of an IFFL circuit among *fos-1a, egl-43a* and *mig-10b* within the FOS-1A transcription network. This IFFL unit may help ensure *mig-10b* expression at the optimal level required for effective AC invasion.

Acknowledgments

We are grateful for the research grants from the National Natural Science Foundation of China (81272559), the Ministry of Education (113044A), and the Ministry of Science and Technology (S2014ZR0340).

Appendix A. Supplementary data

Supplementary data associated with this article can be found, in the online version, at http://dx.doi.org/10.1016/j.bbrc.2014.08.049.

References

[1] A.J. Ridley, M.A. Schwartz, K. Burridge, R.A. Firtel, M.H. Ginsberg, G. Borisy, J.T. Parsons, A.R. Horwitz, Cell migration: integrating signals from front to back, Science 302 (2003) 1704–1709.
[2] P. Friedl, K. Wolf, Tumour-cell invasion and migration: diversity and escape mechanisms, Nat. Rev. Cancer 3 (2003) 362–374.
[3] J.L. Ingram, M.J. Huggins, T.D. Church, Y. Li, D.C. Francisco, S. Degan, R. Firszt, D.M. Beaver, N.L. Lugogo, Y. Wang, M.E. Sunday, P.W. Noble, M. Kraft, Airway fibroblasts in asthma manifest an invasive phenotype, Am. J. Respir. Crit. Care Med. 183 (2011) 1625–1632.
[4] K.H. Lim, Y. Zhou, M. Janatpour, M. McMaster, K. Bass, S.H. Chun, S.J. Fisher, Human cytotrophoblast differentiation/invasion is abnormal in pre-eclampsia, Am. J. Pathol. 151 (1997) 1809–1818.
[5] G.P. Gupta, J. Massague, Cancer metastasis: building a framework, Cell 127 (2006) 679–695.
[6] M. Schoumacher, R.D. Goldman, D. Louvard, D.M. Vignjevic, Actin, microtubules, and vimentin intermediate filaments cooperate for elongation of invadopodia, J. Cell Biol. 189 (2010) 541–556.
[7] D.R. Sherwood, J.A. Butler, J.M. Kramer, P.W. Sternberg, FOS-1 promotes basement-membrane removal during anchor-cell invasion in *C. elegans*, Cell 121 (2005) 951–962.
[8] E.J. Hagedorn, D.R. Sherwood, Cell invasion through basement membrane: the anchor cell breaches the barrier, Curr. Opin. Cell Biol. 23 (2011) 589–596.
[9] J.W. Ziel, E.J. Hagedorn, A. Audhya, D.R. Sherwood, UNC-6 (netrin) orients the invasive membrane of the anchor cell in *C. elegans*, Nat. Cell Biol. 11 (2009) 183–189.
[10] D.R. Sherwood, P.W. Sternberg, Anchor cell invasion into the vulval epithelium in *C. elegans*, Dev. Cell 5 (2003) 21–31.
[11] G.P. Coló, E.M. Lafuente, J. Teixidó, The MRL proteins: adapting cell adhesion, migration and growth, Eur. J. Cell Biol. 91 (2012) 861–868.
[12] C. Chang, C.E. Adler, M. Krause, S.G. Clark, F.B. Gertler, M. Tessier-Lavigne, C.I. Bargmann, MIG-10/Lamellipodin and AGE-1/PI3K promote axon guidance and outgrowth in response to slit and netrin, Curr. Biol. 16 (2006) 854–862.
[13] A.K.H. Stavoe, D.A. Colón-Ramos, Netrin instructs synaptic vesicle clustering through Rac GTPase, MIG-10, and the actin cytoskeleton, J. Cell Biol. 197 (2012) 75–88.
[14] M.A. McShea, K.L. Schmidt, M.L. Dubuke, C.E. Baldiga, M.E. Sullender, A.L. Reis, S. Zhang, S.M. O'Toole, M.C. Jeffers, R.M. Warden, A.H. Kenney, J. Gosselin, M. Kuhlwein, S.K. Hashmi, E.G. Stringham, E.F. Ryder, Abelson interactor-1 (ABI-1) interacts with MRL adaptor protein MIG-10 and is required in guided cell migrations and process outgrowth in *C. elegans*, Dev. Biol. 373 (2013) 1–13.
[15] Z. Wang, Q. Chi, D.R. Sherwood, MIG-10 (Lamellipodin) has netrin-independent functions and is a FOS-1A transcriptional target during anchor cell invasion in *C. elegans*, Development 141 (2014) 1342–1353.
[16] S. Brenner, The genetics of *Caenorhabditis elegans*, Genetics 77 (1974) 71–94.
[17] I. Rimann, A. Hajnal, Regulation of anchor cell invasion and uterine cell fates by the egl-43 Evi-1 proto-oncogene in *Caenorhabditis elegans*, Dev. Biol. 308 (2007) 187–195.
[18] R.S. Kamath, M. Martinez-Campos, P. Zipperlen, A.G. Fraser, J. Ahringer, Effectiveness of specific RNA-mediated interference through ingested double-stranded RNA in Caenorhabditis elegans, Genome Biology 2 (2000). research0002.0001–research0002.0010.
[19] E.J. Hagedorn, H. Yashiro, J.W. Ziel, S. Ihara, Z. Wang, D.R. Sherwood, Integrin acts upstream of netrin signaling to regulate formation of the anchor cell's invasive membrane in *C. elegans*, Dev. Cell 17 (2009) 187–198.
[20] C. Mello, A. Fire, DNA transformation, Methods Cell Biol. 48 (1995) 451–482.
[21] M. Krause, J.D. Leslie, M. Stewart, E.M. Lafuente, F. Valderrama, R. Jagannathan, G.A. Strasser, D.A. Rubinson, H. Liu, M. Way, M.B. Yaffe, V.A. Boussiotis, F.B. Gertler, Lamellipodin, an Ena/VASP ligand, is implicated in the regulation of lamellipodial dynamics, Dev. Cell 7 (2004) 571–583.
[22] E.M. Lafuente, A.A.F.L. van Puijenbroek, M. Krause, C.V. Carman, G.J. Freeman, A. Berezovskaya, E. Constantine, T.A. Springer, F.B. Gertler, V.A. Boussiotis, RIAM, an Ena/VASP and profilin ligand, interacts with Rap1-GTP and mediates Rap1-induced adhesion, Dev. Cell 7 (2004) 585–595.
[23] N. Watanabe, L. Bodin, M. Pandey, M. Krause, S. Coughlin, V.A. Boussiotis, M.H. Ginsberg, S.J. Shattil, Mechanisms and consequences of agonist-induced talin recruitment to platelet integrin αIIbβ3, J. Cell Biol. 181 (2008) 1211–1222.
[24] M.L. Gardel, I.C. Schneider, Y. Aratyn-Schaus, C.M. Waterman, Mechanical integration of actin and adhesion dynamics in cell migration, Annu. Rev. Cell Dev. Biol. 26 (2010) 315–333.
[25] D.Q. Matus, X.-Y. Li, S. Durbin, D. Agarwal, Q. Chi, S.J. Weiss, D.R. Sherwood, In vivo identification of regulators of cell invasion across basement membranes, Sci. Signal. 3 (2010). ra35.
[26] U. Alon, Network motifs: theory and experimental approaches, Nat. Rev. Genet. 8 (2007) 450–461.
[27] D.H. Kim, D. Grun, A. Van Oudenaarden, Dampening of expression oscillations by synchronous regulation of a microRNA and its target, Nat. Genet. 45 (2013) 1337–1344.